

## Dissociation limit and dissociation dynamic of $\text{CF}_4^+$ : Application of threshold photoelectron-photoion coincidence velocity imaging

Xiaofeng Tang, Xiaoguo Zhou<sup>\*</sup>, Manman Wu, Zhi Gao, Shilin Liu, Fuyi Liu, Xiaobin Shan, and Liusi Sheng

Citation: *The Journal of Chemical Physics* **138**, 094306 (2013); doi: 10.1063/1.4792368

View online: <http://dx.doi.org/10.1063/1.4792368>

View Table of Contents: <http://aip.scitation.org/toc/jcp/138/9>

Published by the *American Institute of Physics*

---

### Articles you may be interested in

Dissociation of internal energy-selected methyl bromide ion revealed from threshold photoelectron-photoion coincidence velocity imaging

*The Journal of Chemical Physics* **140**, 044312 (2014); 10.1063/1.4862686

---

**COMPLETELY**

**REDESIGNED!**



**PHYSICS  
TODAY**

*Physics Today* Buyer's Guide  
Search with a purpose.

# Dissociation limit and dissociation dynamic of $\text{CF}_4^+$ : Application of threshold photoelectron-photoion coincidence velocity imaging

Xiaofeng Tang,<sup>1,2</sup> Xiaoguo Zhou,<sup>1,a)</sup> Manman Wu,<sup>1</sup> Zhi Gao,<sup>1</sup> Shilin Liu,<sup>1</sup> Fuyi Liu,<sup>2</sup> Xiaobin Shan,<sup>2</sup> and Liusi Sheng<sup>2</sup>

<sup>1</sup>Hefei National Laboratory for Physical Sciences at the Microscale and Department of Chemical Physics, University of Science and Technology of China, Hefei, Anhui 230026, China

<sup>2</sup>National Synchrotron Radiation Laboratory, University of Science and Technology of China, Hefei, Anhui 230029, China

(Received 7 December 2012; accepted 1 February 2013; published online 1 March 2013)

Dissociation of internal energy selected  $\text{CF}_4^+$  ions in an excitation energy range of 15.40–19.60 eV has been investigated using threshold photoelectron-photoion coincidence (TPEPICO) velocity imaging. Only  $\text{CF}_3^+$  fragment ions are observed in coincident mass spectra, indicating all the  $X^2T_1$ ,  $A^2T_2$ , and  $B^2E$  ionic states of  $\text{CF}_4^+$  are fully dissociative. Both kinetic energy released distribution (KERD) and angular distribution in dissociation of  $\text{CF}_4^+$  ions have been derived from three-dimensional TPEPICO time-sliced images. A parallel distribution of  $\text{CF}_3^+$  fragments along the polarization vector of photon is observed for dissociation of  $\text{CF}_4^+$  ions in all the low-lying electronic states. With the aid of F-loss potential energy curves, dissociation mechanisms of  $\text{CF}_4^+$  ions in these electronic states have been proposed.  $\text{CF}_4^+$  ions in both  $X^2T_1$  and  $A^2T_2$  states directly dissociate to  $\text{CF}_3^+$  and F fragments along the repulsive C-F coordinate, while a two-step dissociation mechanism is suggested for  $B^2E$  state:  $\text{CF}_4^+(B^2E)$  ion first converts to the lower  $A^2T_2$  state via internal conversion, then dissociates to  $\text{CF}_3^+$  and F fragments along the steep  $A^2T_2$  potential energy surface. In addition, an adiabatic appearance potential of  $\text{AP}_0(\text{CF}_3^+/\text{CF}_4)$  has also been established to be  $14.71 \pm 0.02$  eV, which is very consistent with the recent calculated values. © 2013 American Institute of Physics. [<http://dx.doi.org/10.1063/1.4792368>]

## I. INTRODUCTION

As a benchmark molecule with high symmetry, ionization and dissociation of tetrafluoromethane ( $\text{CF}_4$ ) have attracted extensive investigations for a long history. It is well known that its valence-shell electronic configuration in ground state is  $(3a_1)^2(2t_2)^6(4a_1)^2(3t_2)^6(1e)^4(4t_2)^6(1t_1)^6$  with  $T_d$  symmetrical structure,<sup>1</sup> and the Jahn-Teller distortion can reduce its symmetry from  $T_d$  to  $C_{3v}$ . Once removing one  $1t_1$ ,  $4t_2$ , or  $1e$  electron from the outer orbitals,  $\text{CF}_4^+$  ions in various ionic states, e.g.,  $X^2T_1$ ,  $A^2T_2$ , and  $B^2E$ , are produced, respectively. Both  $X^2T_1$  and  $A^2T_2$  bands were structureless in photoelectron spectroscopy (PES)<sup>1–3</sup> and threshold photoelectron spectroscopy (TPES),<sup>4,5</sup> while a few weak vibrational bands superimposed on a broad continuum background were observed for the  $B^2E$  state.<sup>4,5</sup>

In past decades, dissociation of  $\text{CF}_4^+$  ions in the low-lying electronic states has been investigated with many experimental methods, e.g., photoionization,<sup>6,7</sup> electron impact ionization,<sup>8–11</sup> ion-molecule reaction,<sup>12,13</sup> ion imaging,<sup>14</sup> velocity imaging photoionization coincidence (VIPCO),<sup>15</sup> photoelectron fluorescence coincidence,<sup>16,17</sup> photoelectron-photoion coincidence (PEPICO),<sup>18–20</sup> and threshold photoelectron-photoion coincidence (TPEPICO).<sup>5,21,22</sup> Only  $\text{CF}_3^+$  fragment ions were observed for dissociation

of  $\text{CF}_4^+(X^2T_1, A^2T_2, \text{ and } B^2E)$  ions, while no stable  $\text{CF}_4^+$  ions were detected in the most of previous experiments, except that Kime *et al.* observed a very small amount of  $\text{CF}_4^+$  ions using electron impact ionization<sup>10</sup> and Hagenow *et al.* detected  $\text{CF}_4^+$  in dissociative photoionization (DPI) of the dimmer.<sup>23</sup> Therefore, the ground electronic state of  $\text{CF}_4^+$  is generally believed unstable, and both the  $A^2T_2$  and  $B^2E$  excited states can also dissociate along a fragmentation pathway.

As the ground electronic state of  $\text{CF}_4^+$  ions is dissociative in Franck-Condon region, it is very difficult to directly measure the adiabatic appearance potential  $\text{AP}_0(\text{CF}_3^+/\text{CF}_4)$ . When  $\text{CF}_4$  is photoionized in Franck-Condon region, excess energy above the dissociation limit of  $\text{CF}_3^+ + \text{F}$  will be distributed among internal and kinetic energies (KE) of fragments. Thus an upper limit of  $\text{AP}_0(\text{CF}_3^+/\text{CF}_4)$  can be obtained by estimating the released KE from analyzing time-of-flight (TOF) profile of fragments. Using PEPICO technique with He I light source, Brehm *et al.*,<sup>18</sup> Simm *et al.*,<sup>19</sup> and Powis<sup>20</sup>, respectively measured the released KE in dissociation of  $\text{CF}_4^+(X^2T_1)$  ions and proposed the upper limits. By measuring the released KE as a function of excitation energy and assuming that the fractional released KE was independent of ionization energy, Chim *et al.* extrapolated the KE to zero and obtained a lower value of 14.45 eV for  $\text{AP}_0(\text{CF}_3^+/\text{CF}_4)$ .<sup>21</sup> Besides these direct ionization measurements, the  $\text{AP}_0(\text{CF}_3^+/\text{CF}_4)$  value was also derived from thermo-chemical data,<sup>24</sup> ion-molecule reactions<sup>12,13</sup>

<sup>a)</sup> Author to whom correspondence should be addressed. Electronic mail: xzhou@ustc.edu.cn.

TABLE I. Adiabatic appearance potential  $AP_0(\text{CF}_3^+/\text{CF}_4)$  obtained in different experimental measurements and recent quantum chemical calculations.

$AP_0$ (eV)	Experimental/theoretical method	Light source	Reference
Experimental			
$\leq 15.35$	Photoionization efficiency curve	He Hopfield	6
$\leq 14.84 \pm 0.05$	PEPICO	He I	18
$\leq 14.90 \pm 0.1$	PEPICO	He I	19
$\leq 14.7 \pm 0.3$	PEPICO	He I	20
$14.45 \pm 0.20$	TPEPICO	Synchrotron radiation	21
$14.67 \pm 0.04$	Photoionization and thermodynamic	He Hopfield and $\text{H}_2$ continuum	24
$14.24 \pm 0.07$	Ion-molecule reaction	...	12
$14.2 \pm 0.1$	Ion-molecule reaction	...	13
$14.71 \pm 0.02$	TPEPICO velocity imaging	Synchrotron radiation	This work
Theoretical			
$\sim 14.70$	CCSD/Dunning's correlation consistent basis sets <sup>a</sup>	...	25, 27
14.699	W1 and CBS-APNO <sup>b</sup>	...	26

<sup>a</sup>The calculated  $\Delta H_{0\text{K}}(\text{CF}_4)$  and  $\Delta H_{0\text{K}}(\text{CF}_3)$  are  $-927.8$  and  $-464.8$   $\text{kJ} \cdot \text{mol}^{-1}$ , respectively (Ref. 25). The  $IP_{\text{ad}}(\text{CF}_3)$  is  $9.102$  or  $9.001$  eV and thus  $AP_0(\text{CF}_3^+/\text{CF}_4)$  can be calculated as the formula of  $AP_0(\text{CF}_3^+/\text{CF}_4) = \Delta H_{0\text{K}}(\text{CF}_3) + IP_{\text{ad}}(\text{CF}_3) + \Delta H_{0\text{K}}(\text{F}) - \Delta H_{0\text{K}}(\text{CF}_4)$ .

<sup>b</sup>The calculated  $AP_0(\text{CF}_3^+/\text{CF}_4)$  for  $\text{CF}_4 \rightarrow \text{CF}_3^+ + \text{F}$  at W1 and CBS-APNO level using a weighted factor derived from the 0 K appearance energy of H-loss from  $\text{CH}_2\text{F}_2^+$ .

and quantum chemical calculations.<sup>25,26</sup> Table I summarizes the most experimental and recent calculated values of  $AP_0(\text{CF}_3^+/\text{CF}_4)$  and obviously these data are in controversy. Therefore, to establish a more accurate  $AP_0(\text{CF}_3^+/\text{CF}_4)$  in experiment and compare it with the high-level quantum chemical calculated data is a major aim of present work.

For dissociation of  $\text{CF}_4^+$  ions in electronically excited states, an apparent electronic state-selectivity was found in previous investigations. By fitting TOF profile of  $\text{CF}_3^+$  fragment ions, kinetic energy released distribution (KERD) in dissociation of  $\text{CF}_4^+$  ions were evaluated.<sup>5,18–21</sup> Briefly, a nearly monoenergetic kinetic energy was released in dissociation of both  $\text{X}^2\text{T}_1$  and  $\text{A}^2\text{T}_2$  states, on the contrary fragmentation of  $\text{CF}_4^+$  ions in  $\text{B}^2\text{E}$  state showed a wide distribution of released kinetic energy.<sup>18</sup> Furthermore, an induced radiative emission by electron impact was observed and surmised from  $\text{CF}_4^+(\text{B}^2\text{E})$  ion in the van Sprang and Brongersma's experiment.<sup>28</sup> However Maier *et al.* did not detect the expected visible fluorescence of  $\text{B}^2\text{E} \rightarrow \text{X}^2\text{T}_1$  transition in a wavelength range of 200–900 nm.<sup>16</sup> Thus a reasonable explanation is necessary to understand energy redistribution in dissociation of  $\text{B}^2\text{E}$  state. In addition, anisotropic angular distribution of  $\text{CF}_3^+$  fragment ions dissociated from  $\text{CF}_4^+$  ions at fixed excitation energy less than 40 eV was observed recently with the method of ion imaging.<sup>14</sup> However, due to the lack of ionic state-selectivity, the measured  $\text{CF}_3^+$  fragments were produced from dissociation of all energy-allowed electronic states of  $\text{CF}_4^+$  and thus the anisotropic distribution should be a weighted mean of all involved ionic states. Using VIPCO technique, an anisotropic angular distribution of

electrons were also analyzed for photoionization processes to form  $\text{X}^2\text{T}_1$  and  $\text{A}^2\text{T}_2$  ionic states.<sup>15</sup>

To understand dissociation of  $\text{CF}_4^+$  ions in specific ionic state, a few quantum chemistry and dynamics calculations were performed.<sup>29–32</sup> Briefly, both  $\text{X}^2\text{T}_1$  and  $\text{A}^2\text{T}_2$  states are repulsive along the C-F coordinate and able to dissociate to  $\text{CF}_3^+(\text{X}^1\text{A}_1)$  and  $\text{F}(^2\text{P})$  fragments, while the  $\text{B}^2\text{E}$  state is typical bound. These results are generally consistent with the previous experimental conclusions. Moreover, Beärda and Mulder suggested that there is a stable complex of  $\text{CF}_3^+ \dots \text{F}$  along the C-F coordinate of  $\text{X}^2\text{T}_1$  state and hence  $\text{CF}_4^+(\text{X}^2\text{T}_1)$  ions may survive a few vibrations prior to dissociation.<sup>29</sup> However, the lifetime of complex was found extremely short in a direct *ab initio* trajectory calculation.<sup>31</sup>

As an upgraded experimental approach, threshold photoelectron-photoion coincidence (TPEPICO) velocity imaging is powerful to analyze dissociation of energy-selected ions.<sup>33</sup> Compared with the method of fitting TOF profiles, more exact KERD and angular distribution of fragments dissociated from internal energy selected ions can be acquired directly from velocity map images,<sup>34,35</sup> and more details of dissociation dynamics are revealed, e.g., vibrational distribution of fragment ions.<sup>36–39</sup> In the present work, an experimental reinvestigation on dissociative photoionization of  $\text{CF}_4$  in the excitation energy range of 15.40–19.60 eV is performed using TPEPICO velocity imaging. For  $\text{CF}_4^+$  ions in  $\text{X}^2\text{T}_1$ ,  $\text{A}^2\text{T}_2$ , and  $\text{B}^2\text{E}$  states, KERD and angular distributions of  $\text{CF}_3^+$  fragment ions are measured, respectively. An adiabatic appearance potential  $AP_0(\text{CF}_3^+/\text{CF}_4)$  has also been directly obtained in experiment and compared with the recent calculations. More importantly, dissociation mechanisms of specific ionic states of  $\text{CF}_4^+$  are proposed in details with the aid of potential energy curves.

## II. EXPERIMENTS

Present experiments were performed at the U14-A beamline of National Synchrotron Radiation Laboratory (Hefei, China). The configurations of the beamline and TPEPICO velocity imaging spectrometer have been introduced in details previously,<sup>33</sup> and thus only a brief description is presented here. Synchrotron radiation (SR) from an undulator was dispersed with a 6 m spherical-grating monochromator, in which a 370 grooves  $\text{mm}^{-1}$  grating was used to cover a photon energy range of 7.5–22.5 eV. A typical photon bandwidth is 6 meV in this energy range.<sup>40</sup> A gas filter filled with noble gas was used to reduce higher-order harmonic radiation of beamline.

A home-made 30- $\mu\text{m}$ -diameter nozzle was utilized to generate continuous supersonic molecular beam (MB), which interacted with SR at right angle in photoionization chamber. Using a same dc extraction electric field, photoelectrons and photoions produced from DPI process were collected in opposite directions. A specially designed repelling electric field was used to magnify and map velocity image of electrons, and thus the contamination of energetic electrons was almost completely suppressed in TPES and TPEPICO measurement.<sup>33</sup> The typical photoelectron energy resolution is  $\sim 9$  meV. Photoions were projected onto multichannel plates (MCP, 40 mm

diameter) backed by a phosphor screen (Burle Industries, P20). A thermoelectric-cooling charge couple device camera (Andor, DU934N-BV) was used to record ion image on the screen. Once a threshold photoelectron was collected in experiment, a pulsed high voltage (DEI, PVM-4210) was applied at MCPs to act as mass gate, whose time origin and width were decided by TOF of target ion. In the following experiments, a typical 80 ns duration was used to record images of  $\text{CF}_3^+$  fragment ions whose jitter was less than 2 ns. Thus the TPEPICO velocity image of fragment ions dissociated from specific internal energy selected parent ions could be recorded.

Commercial  $\text{CF}_4/\text{Ne}$  (1:9) mixture gas (Nanjing specialty gases) with a stagnation pressure of 2.0 atm was injected into the spectrometer. After collimated by a 0.5-mm-diameter skimmer, MB was intersected with SR at 10 cm downstream from the nozzle. The typical backing pressure in the photoionization chamber was better than  $1 \times 10^{-4}$  Pa with the MB on. The absolute photon energy of SR was carefully calibrated using the well-known ionization energies of noble gases, and a silicon photodiode (International Radiation Detectors Inc., SXUV-100) was used to record photon flux.

### III. RESULTS AND DISCUSSION

#### A. Threshold photoelectron spectrum of $\text{CF}_4$

Threshold photoelectron spectrum of  $\text{CF}_4$  with a step size of 12 meV in an excitation energy range of 15.40–19.60 eV has been measured, normalized to the photon flux, and presented in Fig. 1. Three observed bands are assigned to the lowest-lying three electronic states of  $\text{CF}_4^+$  ions,  $X^2T_1$ ,  $A^2T_2$ , and  $B^2E$ , respectively. The resonant energies and relative intensities of the bands are in good agreement with the previous results.<sup>4,5</sup>  $X^2T_1$  and  $A^2T_2$  bands are broadened and structureless in the spectrum. For  $B^2E$  band, a few weak peaks superimposed over a broadened background in the previous high-resolution TPES<sup>4,5</sup> are indistinct in Fig. 1. Four resonant energies are chosen and noted with stars in Fig. 1, in which two excitation energies within the  $X^2T_1$  band, 15.98 eV and

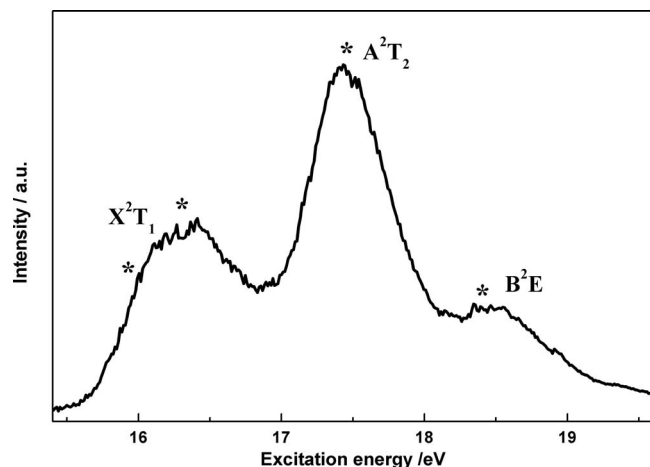


FIG. 1. Threshold photoelectron spectrum of  $\text{CF}_4$  in the excitation energy range of 15.40–19.60 eV.

16.38 eV, are specially selected in order to discuss its dissociation mechanism.

#### B. TPEPICO TOF mass spectra

TPEPICO TOF mass spectra of  $\text{CF}_4$  are measured at photon energies of 15.98, 16.38, 17.54, and 18.48 eV, respectively, and presented in Fig. 2. None  $\text{CF}_4^+$  parent ions is found, and only one TOF peak located at 17.2  $\mu\text{s}$  is observed, which attributes to  $\text{CF}_3^+$  fragment ions. Thus  $\text{CF}_4^+$  ions in all the  $X^2T_1$ ,  $A^2T_2$ , and  $B^2E$  states fully dissociate to produce  $\text{CF}_3^+$  fragment ions, which agrees well with the previous measurements<sup>5,18–20</sup>. Furthermore, the second dissociation limit of  $\text{CF}_3^+(\text{A}^1\text{E}) + \text{F}(^2\text{P})$  is calculated at MP4(FC)/6-311+G(2df,p)//B3LYP/6-611G\* level and 138 kcal·mol<sup>-1</sup> (5.98 eV) higher in energy than that of the lowest  $\text{CF}_3^+(\text{X}^1\text{A}_1) + \text{F}(^2\text{P})$  channel. Since it is beyond the present excitation energy, only the lowest  $\text{CF}_3^+(\text{X}^1\text{A}_1) + \text{F}(^2\text{P})$  channel is taken into account in the following discussion.

With an extraction electric field of 14 V·cm<sup>-1</sup>, the width of TOF profile for ions without kinetic energy released was only about 15 ns (full width at half maximum, FWHM).<sup>33</sup> Due to the kinetic energy release in dissociation of  $\text{CF}_4^+$ , the TOF widths of  $\text{CF}_3^+$  fragment ions in Fig. 2 are obviously broadened to 690, 706, and 760 ns (FWHM) at 15.98, 16.38, and 17.54 eV, respectively. Interestingly, that at 18.48 eV of  $B^2E$  state is only 693 ns although the photon energy far exceeds both  $X^2T_1$  and  $A^2T_2$  ionic states, indicating that dissociative mechanism of  $\text{CF}_4^+(\text{B}^2\text{E})$  ions should be different from that of the  $X^2T_1$  and  $A^2T_2$  states. In addition, the TOF profiles of  $\text{CF}_3^+$  are obviously changed with the photon energy. A near rectangular contour in Figs. 2(a)–2(c) is found for both  $X^2T_1$  and  $A^2T_2$  states, while it shows a triangular shape for  $\text{CF}_3^+$  dissociated from  $\text{CF}_4^+(\text{B}^2\text{E})$  ions at 18.48 eV. Therefore, kinetic energy distribution of  $\text{CF}_3^+$  fragment ions in dissociation of  $X^2T_1$ ,  $A^2T_2$ , and  $B^2E$  states are expected to be different.

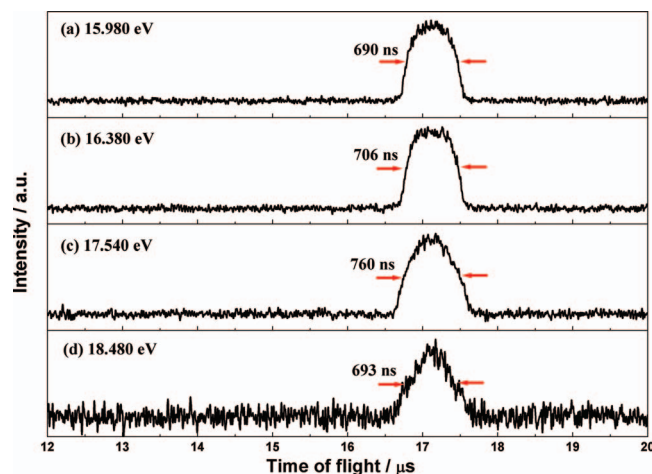


FIG. 2. Threshold photoelectron-photoion coincidence time-of-flight mass spectra for dissociative photoionization of  $\text{CF}_4$  at photon energy of (a) 15.98 eV, (b) 16.38 eV, (c) 17.54 eV, and (d) 18.48 eV.



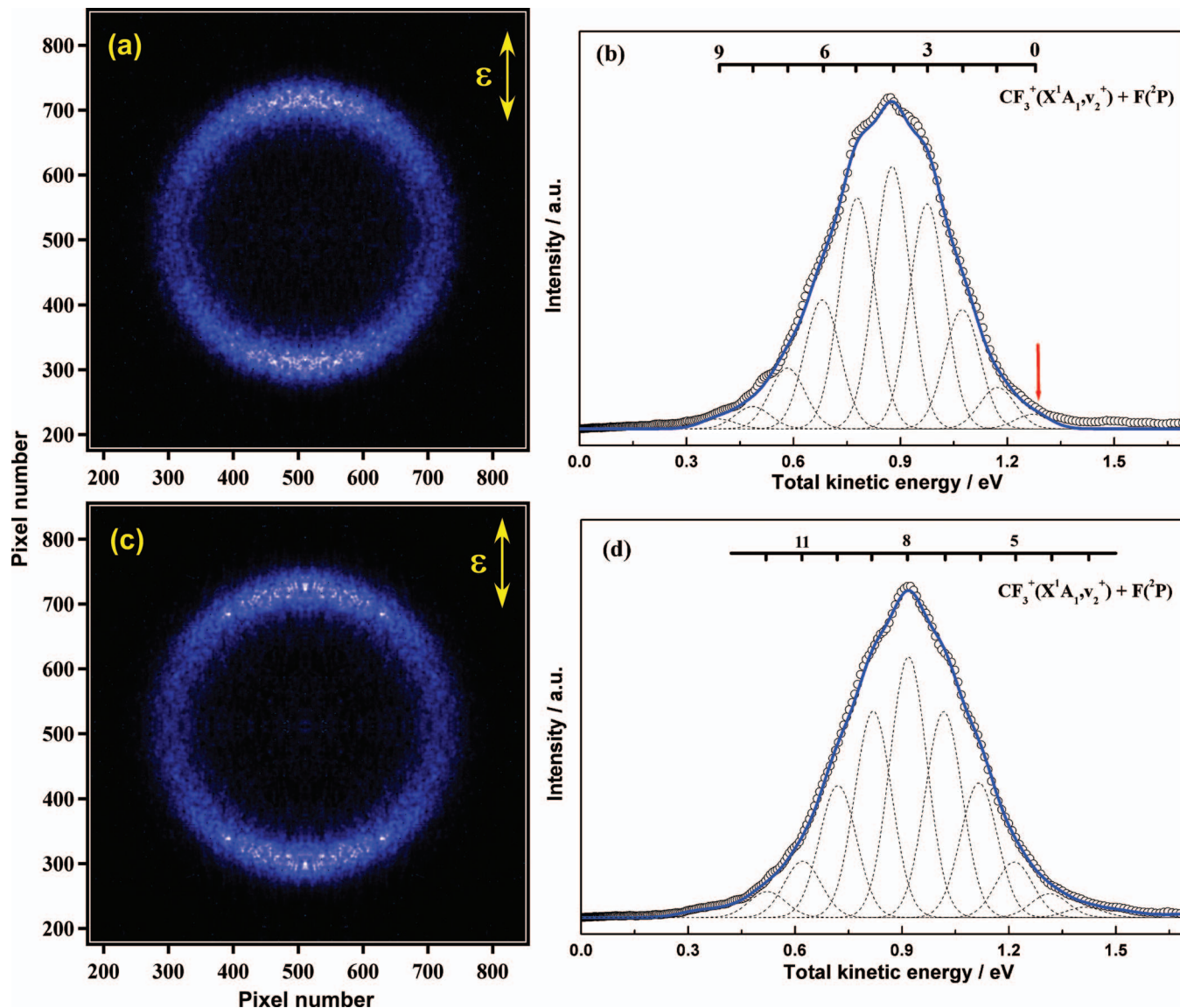


FIG. 3. Three-dimensional threshold photoelectron-photoion coincidence time-sliced velocity images of  $\text{CF}_3^+$  fragments and the corresponding total kinetic energies released distributions in dissociation of  $\text{CF}_4^+(\text{X}^2\text{T}_1)$  ions. (a) and (b) at 15.98 eV; (c) and (d) at 16.38 eV.

### C. TPEPICO velocity images of $\text{CF}_3^+$ dissociated from $\text{CF}_4^+(\text{X}^2\text{T}_1)$ ion

As shown in Table I, the previous measured values of  $\text{AP}_0(\text{CF}_3^+/\text{CF}_4)$  were inconsistent. Especially, the  $\text{AP}_0(\text{CF}_3^+/\text{CF}_4)$  value obtained by Chim *et al.*<sup>21</sup> is far different from the other data,<sup>18–20</sup> although all of them were derived from photoelectron-photoion coincidence measurements. Fortunately, kinetic energy resolution of the present measurement is better than 3% of  $\Delta E/E$  after a careful calibration of ion images using the well-known KERD in dissociation of  $\text{O}_2^+(\text{B}^2\Sigma_g^-)$  ions,<sup>33</sup> and hence more dynamic details in dissociation of  $\text{CF}_4^+(\text{X}^2\text{T}_1)$  ions can be revealed.

Figures 3(a) and 3(c) show the 3D TPEPICO time-sliced velocity images of  $\text{CF}_3^+$  dissociated from the  $\text{CF}_4^+(\text{X}^2\text{T}_1)$  ions at 15.98 eV and 16.38 eV, respectively. The polarization vector  $\epsilon$  of photon is along vertical direction in the image.

There is only one rough ring in both images, indicating that only a nearly monoenergetic distribution is released in dissociation. It is consistent with the previous experiments.<sup>18–20</sup> In addition, a parallel anisotropic distribution can be observed in the images, and thus dissociation of  $\text{CF}_4^+(\text{X}^2\text{T}_1)$  ions should be rapid. By accumulating intensity of the image over angles, speed distribution of  $\text{CF}_3^+$  fragment ions is acquired directly. From conservation of linear momentum, total KERD in dissociation of  $\text{CF}_4^+(\text{X}^2\text{T}_1)$  ions at 15.98 and 16.38 eV can be subsequently obtained and shown in Figs. 3(b) and 3(d). Obviously, the diameter of ring in the images of Figs. 3(a) and 3(c) just slightly increases with excitation energy, and the maximal total kinetic energy of fragments only increases a little bit from 1.28 eV (at 15.98 eV) to 1.40 eV (at 16.38 eV). That means, more fraction of available energy in dissociation has been distributed to internal energy of fragments with

TABLE II. Mean total kinetic energy released ( $\langle E_T \rangle$ ) and anisotropic parameter  $\beta$  in dissociation of  $\text{CF}_4^+$  ions in three low-lying electronic states.

$h\nu$ (eV)	$E_{\text{avail}}$ (eV)	$\langle E_T \rangle$ (eV)	$f_T$		$\beta$	
			Expt.	Theor.	Previous <sup>a</sup>	Present
15.98	1.27	0.85	0.67		...	$0.64 \pm 0.09$
16.38	1.67	0.90	0.54	$0.49^b, 0.65^c$	$0.65 (16.5 \text{ eV})$	$0.72 \pm 0.07$
17.54	2.83	1.20	0.42		$0.60 (17.5 \text{ eV})$	$0.95 \pm 0.08$
18.48	3.77	1.09	0.29		$0.45 (18.5 \text{ eV})$	$0.51 \pm 0.09$

<sup>a</sup>From Ref. 14, where the corresponding excitation energies are shown in parentheses.

<sup>b</sup> $f_T$  is calculated using the classical “impulsive model.”

<sup>c</sup> $f_T$  for dissociation of  $\text{CF}_4^+$  in  $X^2T_1$  state is derived from the direct *ab initio* dynamic calculation at the HF/6-311G(d,p) level in Ref. 31.

excitation energy increasing, which is in agreement with the recent Bodi *et al.*'s experimental conclusion.<sup>41</sup> A unique explanation of the phenomenon is existence of a shallow well on F-loss potential energy surface of  $X^2T_1$  state. Thus the Chim *et al.*'s assumption<sup>21</sup> that the fractional KE released is independent of ionization energy is unreasonable.

Generally, the maximal total kinetic energy of fragments can give an upper limit of adiabatic appearance potential  $\text{AP}_0(\text{CF}_3^+/\text{CF}_4)$ . As indicated in Fig. 3(b), the upper limit should be around 14.7 eV. In the Franck-Condon region,  $\text{CF}_4^+(X^2T_1)$  ions dissociate fast along the C-F bond rupture, and thus the umbrella vibration ( $\nu_2^+ = 798.1 \text{ cm}^{-1}$ )<sup>42,43</sup> of  $\text{CF}_3^+$  is expected to be dominantly excited. Taking into account the total KERD and the upper limit of  $\text{AP}_0(\text{CF}_3^+/\text{CF}_4)$ , the maximal  $\nu_2^+$  quantum number of  $\text{CF}_3^+(X^1A_1)$  should be less than 10 at 15.98 eV. Therefore, the possible vibrational state population of  $\text{CF}_3^+$  can be assigned and shown in Fig. 3(b) as well. In Fig. 3(b), the  $\nu_2^+ = 3-5$  population can be clearly identified, while the other vibrational state populations are blurry in a certain extent due to overlap. Therefore, a typical occurrence of vibrational population reversion is found for  $\text{CF}_3^+$  fragment at 15.98 eV, and the corresponding mean vibrational energy ( $\langle E_v \rangle$ ) is calculated to be 0.43 eV. The most populated vibrational state is located at  $\nu_2^+ = 4$ . Taking the total kinetic energy (1.27 eV) at  $\nu_2^+ = 0$  level as shown with an arrow in Fig. 3(b), the value of  $\text{AP}_0(\text{CF}_3^+/\text{CF}_4)$  is determined to be  $15.98 - 1.27 = 14.71 \text{ eV}$ . According to the kinetic energy resolution is lower than 4 meV ( $1.27 \times 3\% = 3.8 \text{ meV}$ ) and the photoelectron energy resolution

is  $\sim 9 \text{ meV}$ , the uncertainty of  $\text{AP}_0(\text{CF}_3^+/\text{CF}_4)$  can be estimated as less than 20 meV. The present  $\text{AP}_0(\text{CF}_3^+/\text{CF}_4)$  is very consistent with the previous experimental data in Table I<sup>18-20</sup> and exactly matches the value of quantum chemical calculations.<sup>26</sup> In addition, both KERDs in Figs. 3(b) and 3(d) have the similar contours without clear resolvable structures. The most populated vibrational state of  $\text{CF}_3^+$  is changed from  $\nu_2^+ = 4$  at 15.98 eV to  $\nu_2^+ = 8$  at 16.38 eV.

Angular distribution of fragment ions can be derived from the integration of images over a proper range of speed at each angle. Consequently, anisotropic parameter  $\beta$  can be obtained by fitting the angular distribution. At 15.98 and 16.38 eV, both  $\beta$  values for  $\text{CF}_3^+$  fragments are about 0.7 as shown in Table II, which is close to the previous data.<sup>14</sup> Thus dissociation of  $\text{CF}_4^+(X^2T_1)$  ions shows a parallel tendency along the polarization vector.

#### D. TPEPICO velocity image of $\text{CF}_3^+$ dissociated from $\text{CF}_4^+(A^2T_2)$ ion

Because both outer  $1t_1$  and  $4t_2$  molecular orbitals of  $\text{CF}_4$  molecule are consisted of the F lone-pair electron orbitals, characteristics of  $\text{CF}_4^+$  in  $X^2T_1$  and  $A^2T_2$  states are similar. At 17.54 eV,  $\text{CF}_4^+$  ions in the  $A^2T_2$  state are produced and subsequently dissociate to  $\text{CF}_3^+$  and F fragments. The recorded 3D TPEPICO time-sliced velocity image of  $\text{CF}_3^+$  fragments dissociated from  $\text{CF}_4^+(A^2T_2)$  ions is presented in Fig. 4(a). Only the lowest dissociation limit of  $\text{CF}_3^+(X^1A_1) + \text{F}(^2P)$  can be opened at the excitation energy, and a unique rough ring is found in the image. The present image is very similar to the images of Figs. 3(a) and 3(c) indeed, except for its larger diameter.

From the image of Fig. 4(a), the total KERD in dissociation of  $\text{CF}_4^+(A^2T_2)$  ions at 17.54 eV can be obtained and presented in Fig. 4(b). The maximal total kinetic energy of fragments increases to  $\sim 1.9 \text{ eV}$ . Through fitting angular distributions of  $\text{CF}_3^+$  as shown in Fig. 4(c), the corresponding anisotropic parameter  $\beta$  is determined to be 0.95. Therefore, dissociation of  $\text{CF}_4^+$  ions in  $A^2T_2$  state is parallel as well, and moreover the  $A^2T_2$  ionic state has much shorter lifetime than  $X^2T_1$  state. Due to the lack of ionic state-selectivity, Hikosaka

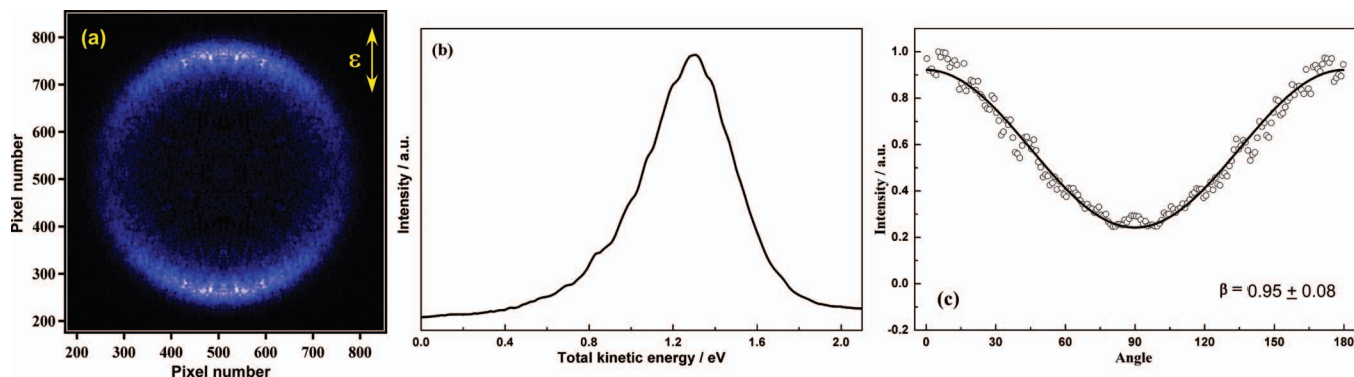


FIG. 4. 3D TPEPICO time-sliced velocity images (a) of  $\text{CF}_3^+$  fragment ions, the corresponding total KERD (b) and angular distributions (c) in dissociation of  $\text{CF}_4^+(A^2T_2)$  ions at 17.54 eV.

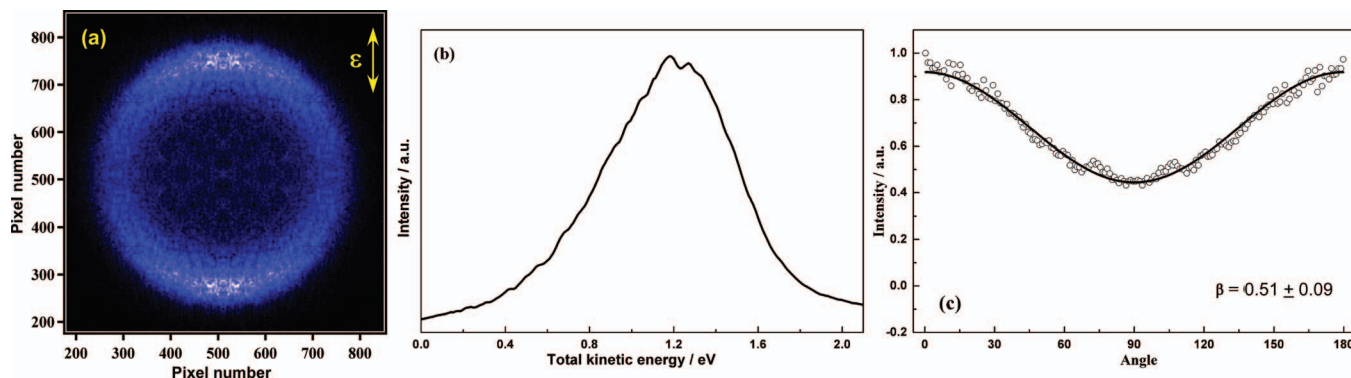


FIG. 5. 3D TPEPICO time-sliced velocity images (a) of  $\text{CF}_3^+$  fragment ions, the corresponding total KERD (b) and angular distributions (c) in dissociation of  $\text{CF}_4^+(\text{B}^2\text{E})$  ions at 18.48 eV.

and Shigemasa<sup>14</sup> obtained a lower value of  $\beta$  ( $\sim 0.6$ ) than ours, and it was closer to it in dissociation of  $\text{X}^2\text{T}_1$  state.

### E. TPEPICO velocity image of $\text{CF}_3^+$ dissociated from $\text{CF}_4^+(\text{B}^2\text{E})$ ion

Figure 5(a) shows the 3D TPEPICO time-sliced velocity image of  $\text{CF}_3^+$  fragments dissociated from  $\text{CF}_4^+(\text{B}^2\text{E})$  ions at 18.48 eV. There is still only one rough ring observed whose width looks much wider than those from both  $\text{X}^2\text{T}_1$  and  $\text{A}^2\text{T}_2$  states, and hence the whole image becomes more diffusive. To our surprise, the maximal total kinetic energy of fragments for  $\text{A}^2\text{T}_2$  and  $\text{B}^2\text{E}$  states are very close and even the most favorable kinetic energy released from  $\text{B}^2\text{E}$  state is slightly lower than that of  $\text{A}^2\text{T}_2$  state as shown in total KERD curves, although the excess energy in dissociation of  $\text{B}^2\text{E}$  state is much larger than that of  $\text{A}^2\text{T}_2$  state. Moreover, the anisotropic parameter  $\beta$  is decreased from 0.95 in  $\text{A}^2\text{T}_2$  state to 0.51 in  $\text{B}^2\text{E}$  state, indicating that the lifetime of  $\text{B}^2\text{E}$  state is longer than those of the lower electronic states,  $\text{X}^2\text{T}_1$  and  $\text{A}^2\text{T}_2$ .

### F. Dissociation mechanism of $\text{CF}_4^+$ in the ground electronic state

Taking the adiabatic appearance potential  $\text{AP}_0(\text{CF}_3^+/\text{CF}_4) = 14.71$  eV, the kinetic and internal energy distributions of  $\text{CF}_3^+$  fragment ions dissociated from  $\text{CF}_4^+$  ions can be derived from the images in Figs. 3–5. The mean total released kinetic energies  $\langle E_T \rangle$  in DPI process at 15.98, 16.38, 17.54, and 18.48 eV, respectively, are calculated and summarized in Table II. The ratios of kinetic energy with available energy,  $f_T$ , can be calculated as 0.67 (15.98 eV), 0.54 (16.38 eV), 0.42 (17.54 eV), and 0.29 (18.48 eV).

If  $\text{CF}_4^+$  ions dissociate fast along the C-F bond rupture with  $\text{C}_{3V}$  geometry, the dissociating time will not enough for intramolecular vibrational redistribution (IVR). Thus the classical “impulsive model” is expected to describe dissociation mechanism,<sup>20</sup> in which the proportion of mean total kinetic energy  $\langle E_T \rangle$  and available energy  $E_{\text{avail}}$  can be calculated using the following formula:

$$f_T = \frac{\langle E_T \rangle}{E_{\text{avail}}} = \frac{\mu_{\text{C-F}}}{\mu_{\text{CF}_3-\text{F}}} = 0.49, \quad (1)$$

where  $\mu$  is reduced mass. In dissociation, the  $\text{C}_{3V}$  geometry of  $\text{CF}_3$  group is initially kept while F atom and  $\text{CF}_3$  recoil sharply and effectively separate in a short time. Then umbrella vibration energy of  $\text{CF}_3^+$  can be distributed from its initial recoiled kinetic energy. As list in Table II, the experimental  $f_T$  for dissociation of  $\text{X}^2\text{T}_1$  state at 15.98 and 16.38 eV are 0.67 and 0.54, respectively, which exactly match the direct *ab initio* dynamic calculations at the HF/6-311G(d,p) level<sup>31</sup> and well compared to the value predicted with the “impulsive model.” Specially, the mean vibrational energy  $\langle E_v \rangle$  of  $\text{CF}_3^+$  fragment ions in DPI process at 15.98 eV is 0.43 eV and high-J rotational excitation of  $\text{CF}_3^+$  is not evident. Therefore, the angle  $\theta$  between the leaving F atom and the  $\text{C}_{3V}$  axis of  $\text{CF}_3^+$  moiety at the moment of dissociation should be about zero, which is also consistent with the conclusion of direct *ab initio* dynamic calculation.<sup>31</sup>

In addition, it is very interesting that  $f_T$  for dissociation of  $\text{X}^2\text{T}_1$  state is slightly decreased with excitation energy increasing as shown in Table II. It is in contrary to a fast dissociation predicted with the classical “impulsive model” along a very steep dissociating potential energy surface, in which the fraction of excess energy is independent on excitation energy. As shown in the schematic F-loss potential energy curves of  $\text{CF}_4^+$  (Fig. 6), a shallow minimum ( $\text{CF}_3^+ \dots \text{F}$

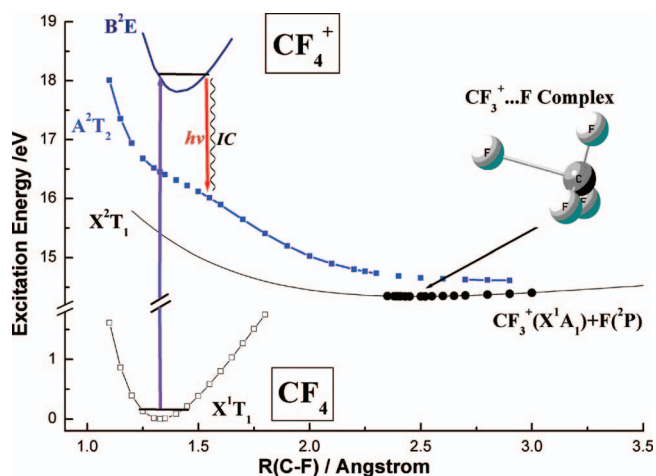


FIG. 6. Schematic F-loss potential energy curves of the low-lying electronic states of  $\text{CF}_4^+$ . The molecular structure of  $\text{CF}_3^+ \dots \text{F}$  complex is calculated at B3LYP/6-311G\* level and shown as well.



complex) on potential energy surface of  $X^2T_1$  ionic state along the C-F bond coordinate was suggested.<sup>29-32</sup> At B3LYP/6-311G\* level, the dissociating C-F bond length of  $CF_3^+ \dots F$  complex is 2.50 Å and the corresponding bond angle  $\theta(F-C-F)$  is 91.55°, which is far away from the Franck-Condon region. The energy of  $CF_3^+ \dots F$  complex is slightly lower (5.29 kcal · mol<sup>-1</sup>) than that of final fragments,  $CF_3^+(X^1A_1) + F(^2P)$ . Although the density functional theory is unsuccessful for dispersive interaction in general, it looks still good for the ground state of  $CF_4^+$  and the present results are in agreement with the high-level *ab initio* calculations.<sup>31</sup> For the  $CF_3^+ \dots F$  complex, the C-F bond length is found at 2.65 Å at MP4SDQ/6-311G(d, p) level, and its binding energy relative to the dissociation limit is 5.8 kcal mol<sup>-1</sup> at the MP4SDQ/6-311G(d,p)//HF/6-311G(d, p) level.<sup>31</sup>

Therefore  $CF_4^+(X^2T_1)$  ions will probably survive a few vibrational periods prior to complete dissociation. Especially in the Franck-Condon allowed lower energy region of  $X^2T_1$  state, e.g., 15.98 eV or even less, the more notable binding interaction of the shallow well cause dissociation more adiabatically, in which the C-F bonds of  $CF_3^+$  fragment are assumed to be infinitely rigid and hence much more excess energy is distributed in translation motion. Thus more fractional KE released is expected for the lower energy  $CF_4^+(X^2T_1)$  ions, which is well consistent with the present experimental conclusions. On the other hand, we need to emphasize that the binding interaction of the complex is too weak to cause dissociating time obviously changed, as implied by the very close  $\beta$  values at 15.98 eV and 16.38 eV.

### G. Dissociation mechanism of $CF_4^+$ in the low-lying electronically excited states

As indicated by both total KERD and angular distribution of fragments, dissociation mechanism of  $CF_4^+$  ions in two low-lying electronically excited states,  $A^2T_2$  and  $B^2E$ , are different. The  $A^2T_2$  state is typical repulsive and adiabatically correlates to the lowest dissociation channel of  $CF_3^+(X^1A_1) + F(^2P)$  (like  $X^2T_1$  state). On the contrary, the  $B^2E$  ionic state is bound and adiabatically correlates with the excited state products, which are energetically inaccessible in the present energy range.

For the  $A^2T_2$  ionic state, the potential energy surface is very steep in the Franck-Condon region and no complex is found along the C-F bond rupture, so that nuclear force drives  $CF_4^+$  ion to dissociate impulsively. As shown in Table II, the fractional KE released is very close to the value predicted with the classical “impulsive model.” Moreover, the measured anisotropic parameter  $\beta$  is 0.95 and larger than that of  $X^2T_1$  state, indicating that dissociation of  $A^2T_2$  state is faster indeed.

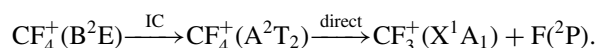
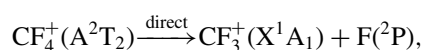
Compared with the cases of the  $X^2T_1$  and  $A^2T_2$  states, dissociation of the  $CF_4^+(B^2E)$  ions is much complicated. As mentioned above, both the mean total released kinetic energy  $\langle E_T \rangle$  and its fraction  $f_T$  of  $B^2E$  state at 18.48 eV are remarkably lower than those of  $A^2T_2$  state at 17.54 eV (in Table II). Additionally, the maximal total kinetic energy of fragment dissociated from  $B^2E$  state is very similar to that

from  $A^2T_2$  state, although the excess energy is much larger. Therefore, partial excess energy of  $B^2E$  state must be released prior to dissociation.

As the  $B^2E$  ionic state is adiabatically bound, its dissociation must occur following internal conversion (IC) or radiative emission to a lower unbound electronic state. Taking into account the Franck-Condon factor, the more favorable unbound lower electronic state is the  $A^2T_2$  state.<sup>20</sup> If  $CF_4^+(B^2E)$  ion undergoes a primary IC process to  $A^2T_2$  state, the high rovibrationally excited ion may be yielded prior to dissociation whose internal energy distribution is far from that through direct photoionization in Franck-Condon region. According to that the dissociating time along the steep  $A^2T_2$  state is only within a few decade femtoseconds, the high rovibrationally excited  $CF_3^+$  fragment can be produced and thus the total kinetic energy released from  $CF_4^+(B^2E)$  is much lower than that along a direct dissociation process. Following a fast dissociation along the steep potential energy surface of  $A^2T_2$ , the invariable  $f_T$  value is expected ( $\sim 0.42$  in Table II) for all vibrationally levels in Franck-Condon region. Therefore the most populated vibrational level of  $A^2T_2$  state after decay of  $CF_4^+(B^2E)$  ion can be estimated. At 18.48 eV ( $B^2E$  state), the measured  $\langle E_T \rangle$  is 1.09 eV as shown in Table II, so that the excess energy prior to dissociation on the  $A^2T_2$  potential energy surface will be  $1.09/0.42 = 2.60$  eV. From energy conservation, the mean released internal energy from  $B^2E$  can be calculated as  $3.77 - 2.60 = 1.17$  eV ( $\sim 1060$  nm), where 3.77 eV is the excess energy at 18.48 eV above dissociation limit. Through the primary IC decay of  $B^2E$  state, the most populated vibrational level of the yielded  $A^2T_2$  state prior to dissociation at 18.48 eV is located at an energy of 17.31 eV (18.48 – 1.17 eV), which is indeed lower than 17.54 eV (direct dissociation of  $A^2T_2$  state as shown in Sec. III D). Thus the mean total released kinetic energy and  $f_T$  at 18.48 eV are certainly lower than those at 17.54 eV, which agrees well with the present measurement.

On the other hand, as van Sprang and Brongersma suggested,<sup>28</sup>  $B^2E$  state is long lived with a lifetime of several nanoseconds, and hence an emission decay of  $CF_4^+(B^2E)$  ion seems also possible.  $CF_4^+(A^2T_2)$  ion will be produced through the  $B^2E \rightarrow A^2T_2$  fluorescence-emission at 18.48 eV. However, as indicated by the present  $\beta$  value (0.51) for dissociation of  $CF_4^+(B^2E)$  ion, the lifetime of  $B^2E$  ionic state should be within picosecond range and much shorter than that suggested by van Sprang and Brongersma.<sup>28</sup> Therefore, emission-dissociation mechanism seems unreasonable and too slow to produce the remarkable anisotropic distribution of  $CF_3^+$  fragment. It should be emphasized that the fluorescence observed by van Sprang and Brongersma<sup>28</sup> could be due to emission of neutral  $CF_3$  or the IR decay of the hot  $CF_3^+$  fragment ion.

Based on the discussion above, the dissociation pathway of electronically excited states,  $A^2T_2$  and  $B^2E$ , can be summarized as follows:





Just to be complete, there is no confessed indication to gain-say fluorescence from B<sup>2</sup>E state up to now. In fact, the expected fluorescence wavelength ( $\sim 1060$  nm) of B<sup>2</sup>E  $\rightarrow$  A<sup>2</sup>T<sub>2</sub> is beyond the wavelength range of detector (200–900 nm) in Maier *et al.*'s experiment, which could cause them to unsuccessfully detect fluorescence.<sup>16</sup> To obtain a firm conclusion of decay mechanism of CF<sub>4</sub><sup>+</sup>(B<sup>2</sup>E) ion, a new photoion fluorescence coincidence experiment is expected.

#### IV. CONCLUSION

Dissociative photoionization of CF<sub>4</sub> via the low-lying ionic electronic states, X<sup>2</sup>T<sub>1</sub>, A<sup>2</sup>T<sub>2</sub>, and B<sup>2</sup>E, has been investigated using TPEPICO velocity imaging. In the excitation energy range of 15.40–19.60 eV, three electronic states are observed in TPES. Only CF<sub>3</sub><sup>+</sup> fragment ions are observed and its TOF profile is appreciably broadened in coincident mass spectra. Interestingly, both the TOF profile contour and width of CF<sub>3</sub><sup>+</sup> fragment ions dissociated from various electronic states are different.

3D TPEPICO time-sliced velocity images of CF<sub>3</sub><sup>+</sup> fragment ions dissociated from specific internal energy selected CF<sub>4</sub><sup>+</sup> ions are recorded at 15.98, 16.38, 17.54, and 18.48 eV, respectively. Both kinetic energy released distribution and angular distribution in dissociation of CF<sub>4</sub><sup>+</sup> ions have been obtained subsequently. For all the electronic states, X<sup>2</sup>T<sub>1</sub>, A<sup>2</sup>T<sub>2</sub>, and B<sup>2</sup>E, the images of CF<sub>3</sub><sup>+</sup> fragments exhibit a parallel distribution along the polarization vector of photon.

For the X<sup>2</sup>T<sub>1</sub> state, it is interesting that the maximal total kinetic energy of fragments only slightly increases from 1.28 eV (at 15.98 eV) to 1.40 eV (at 16.38 eV), indicating that more fractional available energy has been distributed to internal energy of fragments with excitation energy increasing. Thus a shallow minimum (CF<sub>3</sub><sup>+</sup>...F complex) far away from Franck-Condon region is proposed on the potential energy surface of X<sup>2</sup>T<sub>1</sub>, so that CF<sub>4</sub><sup>+</sup>(X<sup>2</sup>T<sub>1</sub>) ions should survive a few vibrational periods prior to complete dissociation. In addition, the vibrational state population of CF<sub>3</sub><sup>+</sup> is assigned by fitting the KERD curves. The most populated vibrational state of CF<sub>3</sub><sup>+</sup> via DPI at 15.98 eV is located at  $v_2^+ = 4$ , while it is increased to  $v_2^+ = 8$  at 16.38 eV. Based on the obtained internal energy distribution of CF<sub>3</sub><sup>+</sup> fragments, an adiabatic appearance potential of AP<sub>0</sub>(CF<sub>3</sub><sup>+</sup>/CF<sub>4</sub>) at  $14.71 \pm 0.02$  eV has been established and is very consistent with the recent calculated values.

For the electronically excited states, dissociation mechanisms of CF<sub>4</sub><sup>+</sup> ions have been proposed with the aid of F-loss potential energy curves. In A<sup>2</sup>T<sub>2</sub> state, CF<sub>4</sub><sup>+</sup> ion dissociates impulsively along the steep potential energy surface to produce CF<sub>3</sub><sup>+</sup> and F fragments, and the corresponding dissociation mechanism is very close to the classical "impulsive model." However, dissociation of the bound B<sup>2</sup>E state is more complicated. The maximal total kinetic energy of fragment dissociated from B<sup>2</sup>E state is very similar to that from A<sup>2</sup>T<sub>2</sub> state, and moreover both  $\langle E_T \rangle$  and  $f_T$  are far lower than those for dissociation of CF<sub>4</sub><sup>+</sup>(A<sup>2</sup>T<sub>2</sub>) ions. Therefore, a two-step dissociation mechanism is suggested as follows: B<sup>2</sup>E state initially converts to the lower A<sup>2</sup>T<sub>2</sub> state via internal conversion,

then CF<sub>4</sub><sup>+</sup> ion dissociates to CF<sub>3</sub><sup>+</sup> and F fragments along the steep potential energy surface of A<sup>2</sup>T<sub>2</sub> state.

#### ACKNOWLEDGMENTS

The financial support is mainly provided by the National Natural Science Foundation of China (NSFC, Grant Nos. 10979042, 21027005, and 21073173) and National Key Basic Research Special Foundation (NKBRFSF, Grant Nos. 2013CB834602 and 2010CB923300). X. Zhou also thanks the Fundamental Research Funds for the Central Universities (Grant No. WK2060030006) and USTC-NSRL Association funding (Grant No. KY2060030007). The China Postdoctoral Science Foundation (Grant No. 2012M511422) supports the work as well.

- <sup>1</sup>C. R. Brundle, M. B. Robin, and H. Basch, *J. Chem. Phys.* **53**, 2196 (1970).
- <sup>2</sup>D. R. Lloyd and P. J. Roberts, *J. Electron. Spectrosc. Relat. Phenom.* **7**, 325 (1975).
- <sup>3</sup>D. M. P. Holland, A. W. Potts, A. B. Trofimov, J. Breidbach, J. Schirmer, R. Feifel, T. Richter, K. Godehusen, M. Martins, A. Tutay, M. Yalcinkaya, M. Al-Hada, S. Eriksson, and L. Karlsson, *Chem. Phys.* **308**, 43 (2005).
- <sup>4</sup>A. J. Yench, A. Hopkirk, A. Hiraya, G. Dujardin, A. Kvaran, L. Hellner, M. J. Besnard-Ramage, R. J. Donovan, J. G. Goode, R. R. J. Maier, G. C. King, and S. Spyrou, *J. Electron. Spectrosc. Relat. Phenom.* **70**, 29 (1994).
- <sup>5</sup>J. C. Creasey, H. M. Jones, D. M. Smith, R. P. Tuckett, P. A. Hatherly, K. Codling, and I. Powis, *Chem. Phys.* **174**, 441 (1993).
- <sup>6</sup>T. A. Walter, C. Lifshitz, W. A. Chupka, and J. Berkowitz, *J. Chem. Phys.* **51**, 3531 (1969).
- <sup>7</sup>J. C. Creasey, I. R. Lambert, R. P. Tuckett, K. Codling, L. J. Frasiniski, P. A. Hatherly, M. Stankiewicz, and D. M. P. Holland, *J. Chem. Phys.* **93**, 3295 (1990).
- <sup>8</sup>K. Stephan, H. Deutsch, and T. D. Märk, *J. Chem. Phys.* **83**, 5712 (1985).
- <sup>9</sup>H. Deutsch, K. Leiter, and T. D. Märk, *Int. J. Mass Spectrom. Ion Process.* **67**, 191 (1985).
- <sup>10</sup>Y. J. Kime, D. C. Driscoll, and P. A. Dowben, *J. Chem. Soc. Faraday Trans. II* **83**, 403 (1987).
- <sup>11</sup>W. Z. Zhang, G. Cooper, T. Ibuki, and C. E. Brion, *Chem. Phys.* **137**, 391 (1989).
- <sup>12</sup>E. R. Fisher and P. B. Armentrout, *Int. J. Mass Spectrom. Ion Process.* **101**, R1 (1990).
- <sup>13</sup>M. Tichy, G. Javahery, N. D. Twiddy, and E. E. Ferguson, *Int. J. Mass Spectrom. Ion Process.* **79**, 231 (1987).
- <sup>14</sup>Y. Hikosaka and E. Shigemasa, *J. Electron. Spectrosc. Relat. Phenom.* **152**, 29 (2006).
- <sup>15</sup>T. Kinugawa, Y. Hikosaka, A. M. Hodgekins, and J. H. D. Eland, *J. Mass Spectrom.* **37**, 854 (2002).
- <sup>16</sup>J. P. Maier and F. Thommen, *Chem. Phys. Lett.* **78**, 54 (1981).
- <sup>17</sup>H. Biehl, K. J. Boyle, D. M. Smith, and R. P. Tuckett, *Chem. Phys.* **214**, 357 (1997).
- <sup>18</sup>B. Brehm, R. Frey, A. Küstler, and J. H. D. Eland, *Int. J. Mass Spectrom. Ion Phys.* **13**, 251 (1974).
- <sup>19</sup>I. G. Simm, C. J. Danby, J. H. D. Eland, and P. I. Mansell, *J. Chem. Soc. Faraday Trans. II* **72**, 426 (1976).
- <sup>20</sup>I. Powis, *Mol. Phys.* **39**, 311 (1980).
- <sup>21</sup>R. Y. L. Chim, R. A. Kennedy, R. P. Tuckett, W. D. Zhou, G. K. Jarvis, C. A. Mayhew, D. J. Collins, and P. A. Hatherly, *Surf. Rev. Lett.* **9**, 129 (2002).
- <sup>22</sup>G. A. Garcia, H. Soldi-Lose, and L. Nahon, *Rev. Sci. Instrum.* **80**, 023102 (2009).
- <sup>23</sup>G. Hagenow, W. Denzer, B. Brutschy, and H. Baumgärtel, *J. Phys. Chem.* **92**, 6487 (1988).
- <sup>24</sup>R. L. Asher and B. Ruscic, *J. Chem. Phys.* **106**, 210 (1997).
- <sup>25</sup>J. Csontos, Z. Rolik, S. Das, and M. Kállay, *J. Phys. Chem. A* **114**, 13093 (2010).
- <sup>26</sup>A. Bodi, A. Kvaran, and B. Sztáray, *J. Phys. Chem. A* **115**, 13443 (2011).
- <sup>27</sup>H. Dossmann, G. A. Garcia, L. Nahon, B. K. C. de Miranda, and C. Alcaraz, *J. Chem. Phys.* **136**, 204304 (2012).
- <sup>28</sup>H. A. Van Sprang, H. H. Brongersma, and F. J. De Heer, *Chem. Phys.* **35**, 51 (1978).

- <sup>29</sup>R. A. Beärda and J. J. C. Mulder, *Chem. Phys.* **128**, 479 (1988).
- <sup>30</sup>R. A. Beärda, H. R. R. Wiersinga, J. F. M. Aarts, and J. J. C. Mulder, *Chem. Phys.* **137**, 157 (1989).
- <sup>31</sup>H. Tachikawa, *J. Phys. B* **33**, 2367 (2000).
- <sup>32</sup>J. M. G. de la Vega and E. San Fabián, *Chem. Phys.* **151**, 335 (1991).
- <sup>33</sup>X. F. Tang, X. G. Zhou, M. L. Niu, S. L. Liu, J. D. Sun, X. B. Shan, F. Y. Liu, and L. S. Sheng, *Rev. Sci. Instrum.* **80**, 113101 (2009).
- <sup>34</sup>H. Wang, X. G. Zhou, S. L. Liu, B. Jiang, D. X. Dai, and X. M. Yang, *J. Chem. Phys.* **132**, 244309 (2010).
- <sup>35</sup>H. F. Xu, Y. Guo, S. L. Liu, X. X. Ma, D. X. Dai, and G. H. Sha, *J. Chem. Phys.* **117**, 5722 (2002).
- <sup>36</sup>X. F. Tang, X. G. Zhou, M. L. Niu, S. L. Liu, and L. S. Sheng, *J. Phys. Chem. A* **115**, 6339 (2011).
- <sup>37</sup>X. F. Tang, M. L. Niu, X. G. Zhou, S. L. Liu, F. Y. Liu, X. B. Shan, and L. S. Sheng, *J. Chem. Phys.* **134**, 054312 (2011).
- <sup>38</sup>X. F. Tang, X. G. Zhou, M. M. Wu, S. L. Liu, F. Y. Liu, X. B. Shan, and L. S. Sheng, *J. Chem. Phys.* **136**, 034304 (2012).
- <sup>39</sup>X. F. Tang, X. G. Zhou, M. M. Wu, Y. Cai, S. L. Liu, and L. S. Sheng, *J. Phys. Chem. A* **116**, 9459 (2012).
- <sup>40</sup>S. S. Wang, R. H. Kong, X. B. Shan, Y. W. Zhang, L. S. Sheng, Z. Y. Wang, L. Q. Hao, and S. K. Zhou, *J. Synchrotron Radiat.* **13**, 415 (2006).
- <sup>41</sup>A. Bodi, P. Hemberger, T. Gerber, and B. Sztáray, *Rev. Sci. Instrum.* **83**, 083105 (2012).
- <sup>42</sup>Y. Pak and R. C. Woods, *J. Chem. Phys.* **106**, 6424 (1997).
- <sup>43</sup>M. E. Jacox, *J. Phys. Chem. Ref. Data* **27**, 115 (1998).